Journal of Alloys and Compounds 513 (2012) 266–272

Contents lists available at SciVerse ScienceDirect

Journal of Alloys and Compounds

journal homepage: www.elsevier.com/locate/jallcom

Cobalt borate catalysts for hydrogen production via hydrolysis of sodium borohydride

A.M. Ozerova, V.I. Simagina, O.V. Komova*, O.V. Netskina, G.V. Odegova, O.A. Bulavchenko, N.A. Rudina

Boreskov Institute of Catalysis, Pr. Akademika Lavrentieva 5, Novosibirsk 630090, Russian Federation

ARTICLE INFO

Article history:
Received 13 July 2011
Received in revised form 11 October 2011
Accepted 12 October 2011
Available online 20 October 2011

Keywords:
Cobalt borate
Cobalt boride
Sodium borohydride
Hydrolysis

ABSTRACT

Cobalt borides are known to be active catalysts in $NaBH_4$ hydrolysis. *In situ* generation of the active cobalt boride phase in sodium borohydride aqueous solutions is accompanied by formation of cobalt borate whose contribution to the overall catalytic activity of the system has not been studied in detail. In this work an amorphous phase of cobalt borate, which transforms to $Co_2B_2O_5$ upon crystallization, has been synthesized and analyzed. As-synthesized cobalt borate shows high activity in $NaBH_4$ hydrolysis due to its reduction resulting in catalytically active cobalt-containing phase.

1. Introduction

Hydrogen storage and conversion are essential for the emerging hydrogen economy. One of the important research areas of today is to identify the most effective hydrogen storage materials. Several complex hydrides, including $NaBH_4$, $LiBH_4$, $NaAlH_4$, $Mg(BH_4)_2$, and NH_3BH_3, have been found to be potentially suitable for hydrogen storage because of their high hydrogen storage capacity [1,2]. Sodium borohydride, $NaBH_4$, in particular, is the focus of interest since the late 1990s because of its stability in alkaline solutions, non-flammability, non-toxicity, environmental safety and the high theoretical hydrogen content [3–5]. It is also the least expensive metal hydride readily available commercially, and it is currently one of the best candidates for use in portable devices [6].

At ambient temperature the complete hydrolysis of sodium borohydride takes place only in the presence of a suitable catalyst:

$$NaBH_4 + 2H_2O \xrightarrow{cat} NaBO_2 + 4H_2 \tag{1}$$

The composition of the sodium borate may vary depending on the process conditions. Several sodium borate species have been identified, including $NaBO_2{\cdot}xH_2O$ ($x = 2, 4$) and $Na_2B_4O_7{\cdot}xH_2O$ ($x = 5, 10$) [7–9].

There have been many efforts to improve catalytic systems for $NaBH_4$ hydrolysis. Catalysts containing noble metals (Pt, Rh, Ru) have shown the best performance in this process [10–12], but their high cost makes them prohibitive for wider applications. Cobalt-based catalysts have recently emerged to potentially replace noble metals in $NaBH_4$ hydrolysis [13], including Co nanoparticles [14–16], metallic cobalt [7,17], cobalt salts [7,8,17,18], cobalt oxides [16,18–20], Co–B hollow spheres [21], and supported Co-containing catalysts [22–26]. However, most of the work in this area has been devoted to cobalt boride, Co_xB, either in its pure form [27–31] or with dopants (Ni, Fe, Cu, W, Cr, Mo, Mn, and P) [25,32–35].

There are two synthetic approaches to prepare a catalytically active cobalt boride phase, *ex situ* and *in situ*. In the *ex situ* preparation common cobalt salts are reduced with a $NaBH_4$ solution followed by separation, washing, and drying of the black Co_xB precipitate [27–31]. In the *in situ* route the active boride phase is obtained from cobalt compounds directly in the medium of $NaBH_4$ hydrolysis reaction [7,8,17,18]. The latter approach simplifies considerably the catalyst preparation procedure. In both cases the reduction process can be described as follows:

$$CoCl_2 + 4NaBH_4 + 9H_2O \rightarrow Co_2B + 4NaCl + 12.5H_2 + 3B(OH)_3 \tag{2}$$

The final composition of products forming in the reaction of sodium borohydride with cobalt salts in aqueous solutions greatly depend on the reaction conditions, such as reagent concentrations, the order of their mixing, pH of the solution, washing and drying procedures, and the storage conditions [36,37]. Along with the amorphous Co_xB phases ($x = 1 \div 3$) some other phases may form as well, such as metallic cobalt and amorphous cobalt borate. The latter is most likely the result of interaction of cobalt ions with

---

* Corresponding author. Tel.: +7 3832 3307458; fax: +7 3832 3307336.
E-mail address: komova@catalysis.ru (O.V. Komova).

0925-8388/$ – see front matter © 2011 Elsevier B.V. All rights reserved.
doi:10.1016/j.jallcom.2011.10.033

by-products of sodium borohydride hydrolysis which, according to Glavee et al. [36], can be expressed as

$$Co^{2+} + 2NaBO_2 \rightarrow 2Na^+ + Co(BO_2)_2 \qquad (3)$$

Transmission electron microscopy (TEM) studies of Co_xB particles formed *in situ* in the presence of $NaBH_4$ indicated that they had almost always been covered in a layer of oxygen-containing cobalt and boron compounds [8,13,14,37]. After calcination of these particles, a $Co_2B_2O_5$ phase had been found among the crystallization products [8] suggesting that the amorphous phase of cobalt borate was present in the sample before calcination. While the catalytic behavior of Co_xB is well known, questions remain on how the presence of amorphous cobalt borate will affect the $NaBH_4$ hydrolysis, since the catalytic activity of cobalt borate in this reaction has not been studied. If this effect is unfavorable, a procedure should be developed to minimize the amount of amorphous cobalt borate in Co–B catalysts.

The purpose of this work has been to synthesize an individual phase of amorphous cobalt borate, Co–B–O, similar to that found in Co–B catalysts, and to compare its catalytic activity in sodium borohydride hydrolysis with other cobalt compounds.

2. Experimental

2.1. Chemicals

All commercial chemical reagents were used as received, including sodium borohydride, $NaBH_4$ (Acros Organics, 98 wt.%), cobalt (II) chloride hexahydrate, $CoCl_2{\cdot}6H_2O$ (GOST 4525-77), cobalt (II) nitrate hexahydrate, $Co(NO_3)_2{\cdot}6H_2O$ (GOST 4528-78), cobalt (II, III) oxide, Co_3O_4 (GOST 4467-79), cobalt (II) oxide, CoO (GOST 18671-73), cobalt (II) carbonate hydrate, $2CoCO_3{\cdot}3Co(OH)_2{\cdot}H_2O$ (GOST 5407-78), sodium hydroxide, NaOH (GOST 4328-77), hydrogen peroxide, H_2O_2 (GOST 10929-76), urea, $CO(NH_2)_2$ (GOST 2081-92), and acetone, CH_3COCH_3 (GOST 2603-79).

2.2. Sample preparation

The Co–B–O sample was synthesized using a modified version of the method developed by Glavee et al. [36]. The procedure is based on the interaction of cobalt chloride with sodium borate in an aqueous solution as follows. A solution of $CoCl_2{\cdot}6H_2O$ (0.305 M, 200 ml) was added drop-wise to a solution of sodium borate (0.61 M, 200 ml) at room temperature under stirring which resulted in instantaneous formation of a pink suspension. The solid Co–B–O product was filtered off, thoroughly washed with distilled water, and dried in air at room temperature. We observed that during washing the color of precipitate changed from pink to purple.

The solution of sodium borate used in the synthesis of Co–B–O was prepared as follows. A solution of $NaBH_4$ (0.12 M, 1200 ml) was subjected to hydrolysis with $CoCl_2{\cdot}6H_2O$ (1.404 g) at 40 °C under mechanical stirring. After the hydrolysis reaction was complete the sodium borate solution was separated from the catalyst and evaporated to the required concentration. A portion of the solution was evaporated until crystals of sodium borate precipitated which were then separated from the mother liquor, dried in a vacuum box at 80 °C for 3 h and studied by FTIR spectroscopy.

The CoOOH sample was prepared by the precipitation-oxidation method in an aqueous solution as described in [38]. The precipitation process was carried out at 50 °C via a drop-wise addition of a solution of $Co(NO_3)_2{\cdot}6H_2O$ (0.6 M, 50 ml) to a solution of NaOH (3.2 M, 100 ml) under constant stirring. 100 ml of H_2O_2 (50 wt.%) was then added drop-wise to the reaction mixture under stirring. The solid product was filtered off, thoroughly washed with distilled water and dried at 65 °C in air for 26 h. The resulting product was analyzed with XRD which confirmed it as the pure CoOOH phase (JCPDS PDF card no. 26-1107).

The sample of $CoCO_3{\cdot}Co(OH)_2{\cdot}0.22H_2O$ (JCPDS PDF card no. 48-0083) was prepared by homogeneous precipitation [39]. 500 ml of a solution containing $Co(NO_3)_2{\cdot}6H_2O$ (0.1 M) and $CO(NH_2)_2$ (1 M) was heated to 85 °C and kept at this temperature for 3 h under constant stirring. The solid product obtained was filtered off, thoroughly washed with distilled water and dried at 110–130 °C in air for 7 h.

2.3. Sample characterization

The morphology of the Co–B–O sample was studied by scanning electron microscopy (SEM) using a JSM 6460LV microscope (JEOL, Japan).

Bulk concentrations of Co and B in the studied samples were determined by inductively coupled plasma atomic emission spectrometry using an Optima 4300 DV instrument.

The diffuse reflectance electronic spectra of the Co–B–O sample were measured in air at room temperature on a Specord M40 spectrophotometer (Carl Zeiss, Jena) equipped with a standard diffuse reflectance attachment in the region of 200–900 nm.

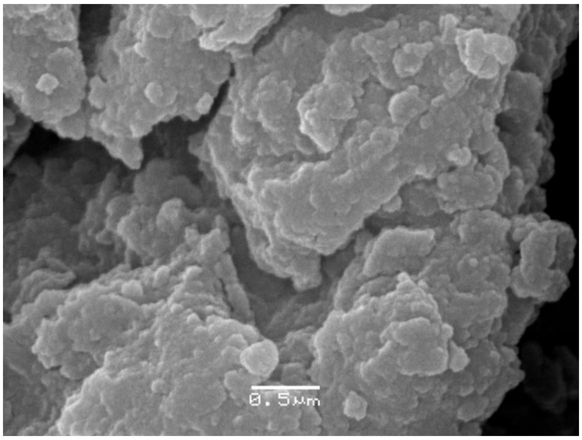

Fig. 1. SEM image of the Co–B–O sample.

FTIR spectra were recorded in air at room temperature on a Bomen MB-102 Fourier spectrometer. For FTIR analysis samples were compressed into thin wafers with cesium iodide, CsI.

Thermal analysis was performed on a STA 449C Jupiter instrument in a flow of helium (10 ml/min) at temperatures from 25 to 1000 °C and the heating rate of 10 °C/min.

The high-temperature diffraction studies were performed using a D8 diffractometer (Bruker, Germany) using a high-temperature X-ray chamber (Anton Paar, Austria). The instrument was equipped with a Gebel mirror (Bruker, Germany) which formed a parallel X-ray beam. Cu Kα radiation with a wave length of $\lambda = 1.5418$ Å was used. The measurements were carried out at a residual pressure of 5×10^{-6} bar in the range of angles from 15° to 70° in steps of 0.05°. The collection time was from 5 to 20 s.

2.4. Hydrogen generation experiments

Hydrogen generation experiments were carried out at 40 °C in a temperature-controlled glass internal mixing reactor equipped with a magnetic stirrer at 800 rpm. A freshly prepared aqueous solution of $NaBH_4$ (1.2 mmol, 10 ml) was placed into the reactor. The known amount of catalyst (0.0117 g) was then added and the volume of produced hydrogen gas was measured with a 100 ml gas burette with a resolution of 0.2 ml. The data obtained were corrected to N.T.P. Based on three repeated experiments under the same conditions the experimental uncertainty was less than 5%.

The following catalysts were studied, Co–B–O, $CoCl_2{\cdot}6H_2O$, Co_3O_4, CoO, CoOOH, $CoCO_3{\cdot}Co(OH)_2{\cdot}0.22H_2O$, $2CoCO_3{\cdot}3Co(OH)_2{\cdot}H_2O$. When necessary, after the catalytic reaction was complete the catalysts were separated from the reaction medium by a magnet, rapidly washed with acetone, and dried at 80 °C for 3 h under vacuum, and then studied by a set of physical methods.

The long-term cyclic stability of catalysts was tested by repeating the above procedure of $NaBH_4$ hydrolysis. After the first portion of $NaBH_4$ (1.2 mmol, 10 ml) was fully converted, a fresh portion of solid $NaBH_4$ (1.2 mmol) was added to the reactor.

3. Results and discussion

3.1. Characterization of the Co–B–O sample

To prepare the Co–B–O sample the synthesis conditions were chosen as close as possible to the experimental conditions of the catalytic hydrolysis of $NaBH_4$ over cobalt chloride. To this effect the sodium borate solution used in the Co–B–O synthesis was made not by dissolving a commercial sodium borate reagent, but instead the solution was used which was left after $NaBH_4$ hydrolysis by $CoCl_2$ (see Section 2). When thus prepared sodium borate solution was allowed to react with $CoCl_2$ a pink-to-purple Co–B–O precipitate was formed; the purple color is indicative of several types of cobalt borates as described in the literature [40–42].

The dried Co–B–O sample was X-ray amorphous. As shown in Fig. 1, SEM images revealed that the Co–B–O sample was composed of dense irregular particles tens to hundreds micrometers

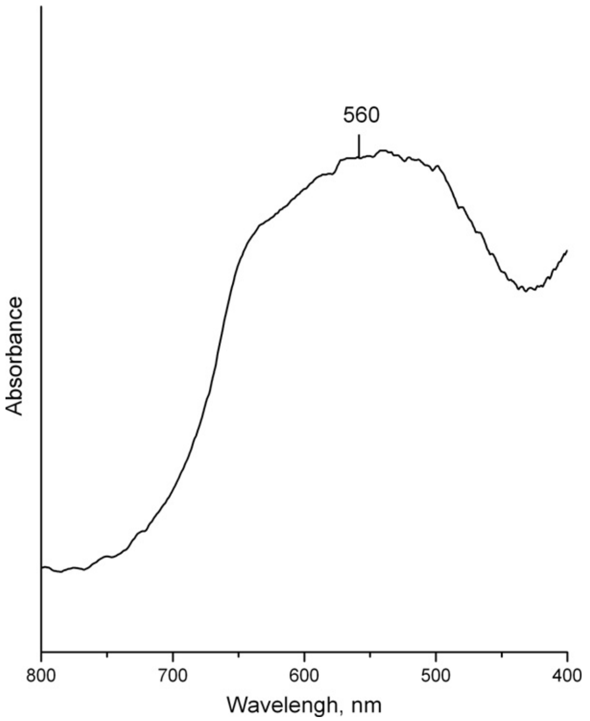

Fig. 2. Diffuse reflectance electronic spectrum of the Co–B–O sample.

in size, with bigger particles consisting of smaller scale-shaped particles. The chemical analysis indicated that the sample contained 37.00 wt.% Co and 7.41 wt.% B which corresponds to the molar ratio Co:B = 1:1.09. The sodium content in the sample was less than 0.01 wt.%. Based on this chemical composition and the TG-DTA data (see below), the chemical formula of the Co–B–O sample can be expressed as $2CoO{\cdot}B_2O_3{\cdot}4H_2O$, using a nomenclature traditionally used for metal borates. The amorphous cobalt borate phase obtained by Glavee et al. under similar experimental conditions [36] was identified as $Co(BO_2)_2$ (molar ratio Co:B = 1:2). The lower molar ratio obtained in our case was most likely due to polymerization and association of borate ions in aqueous solution [40].

Fig. 2 shows a diffuse reflectance electronic spectrum of the as-synthesized Co–B–O sample in the region of d-d transitions of cobalt ions. In this spectral region there is a broad absorption band with a maximum at 560 nm. Similar absorption was observed in [41] for the amorphous $Co_2B_2O_5$ phase where it was attributed to d–d transitions of Co^{2+} ions in the distorted octahedral coordination.

FTIR spectra of the as-synthesized Co–B–O sample and of the sodium borate prepared via evaporating the solution after $NaBH_4$ hydrolysis (see Section 2) are presented in Fig. 3. A direct comparison of the observed sodium borate spectrum with those of other borates [43,44] by its position, shape and the half-width of absorption bands, indicates that this spectrum most closely resembles $Na_2B_4O_7{\cdot}xH_2O$. The band at 3475 cm^{-1} corresponds to the valence vibrations of O–H groups. The band at 1635 cm^{-1} is characteristic of the deformational vibrations of H–O–H indicating the presence of water. The bands at 1359 cm^{-1} and 883 cm^{-1} are due to asymmetric and symmetric vibrations in the $B_{(3)}$–O group. And the bands at 1027 cm^{-1} and 736 cm^{-1} are due to asymmetric and symmetric vibrations in the $B_{(4)}$–O group. The presence of three- and four-coordinated boron species is consistent with the structure of hydrated sodium tetraborate, where polyborate anions, $[B_4O_5(OH)_4]^{2-}$, are known to contain two trigonal BO_3 groups and two tetragonal BO_4 groups [43]. Moreover, $Na_2B_4O_7{\cdot}xH_2O$ (x = 5, 10) was reported among products of $NaBH_4$ hydrolysis [7,9]. In the FTIR spectrum of Co–B–O the observed coordination of borate anions appears to be identical to that of $[B_4O_5(OH)_4]^{2-}$.

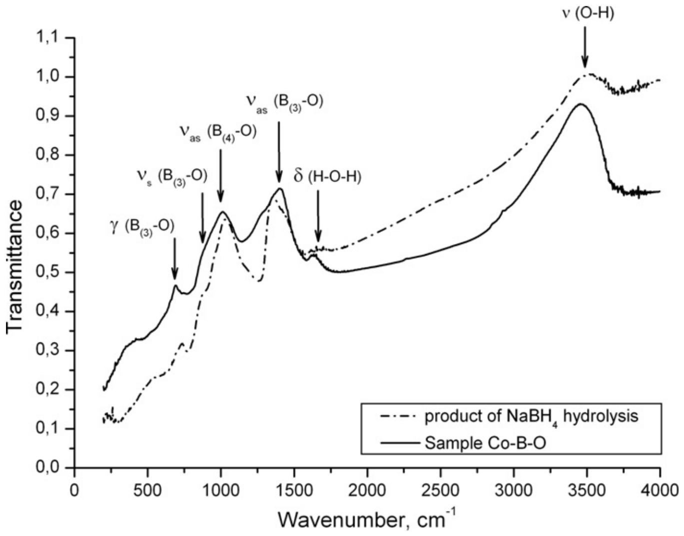

Fig. 3. FTIR spectra of sodium borate remaining after hydrolysis of $NaBH_4$ and of the Co–B–O sample.

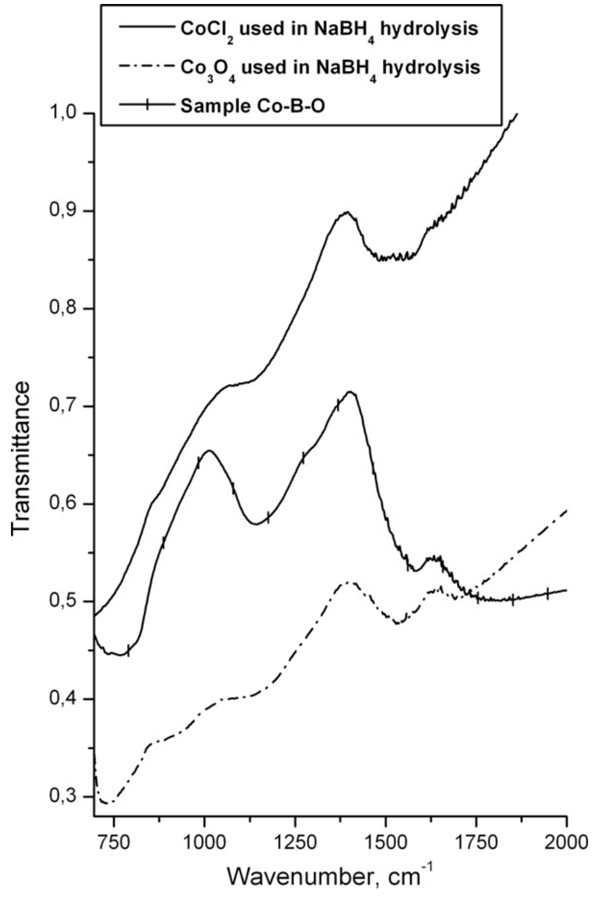

Fig. 4. FTIR spectra of the cobalt boride catalysts formed *in situ* via hydrolysis of $NaBH_4$ using $CoCl_2$ and Co_3O_4.

IR absorption bands due to B–O bond vibrations have been also observed in the IR spectra of catalysts formed *in situ* during $NaBH_4$ hydrolysis with $CoCl_2$ and Co_3O_4 (Fig. 4). Similar IR absorption bands were reported previously for other cobalt boride systems,

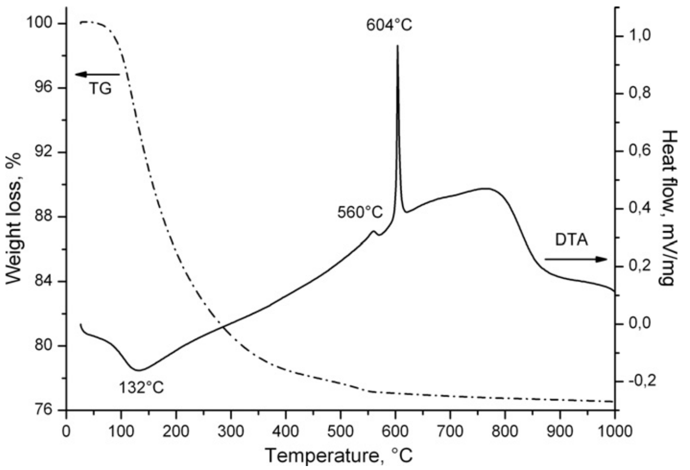

Fig. 5. TG-DTA curves for the Co–B–O sample.

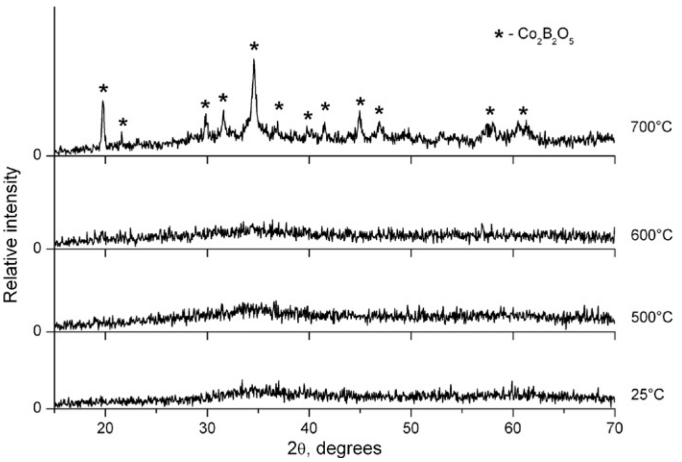

Fig. 6. XRD patterns acquired after vacuum treatment of the Co–B–O sample at 25, 500, 600 and 700 °C.

where they were tentatively attributed to surface-adsorbed borate anions [13,29,45]. However this earlier attribution may not be entirely correct. Judging by high intensity of absorption bands in the borate anion absorption region this IR pattern is most likely an indication of the amorphous cobalt borate phase expected to form in these samples [8,36]. Possible presence of such amorphous phases should be taken into consideration in further studies of any relationships between their catalytic activity and composition.

Thermal TG-DTA analysis of the Co–B–O sample provides an additional insight into its nature and the underlying structure. Our results are in agreement with the results previously reported for a hydrated form of amorphous cobalt borate [40,46]. An endothermic peak at 132 °C can be seen in the TG-DTA curves presented in Fig. 5. This peak corresponds to desorption of significant amounts of structural water and is accompanied by a mass loss as high as 22.15 wt.%, or 4 water molecules per $2CoO{\cdot}B_2O_3$, in agreement with the results of the chemical analysis (see above). Further heating leads to two exothermic maxima, a small one at 560 °C and a rather large maximum at 604 °C, while the mass loss remains almost negligible, only 1.3 wt.%. Such strong exothermic effects during crystallization are believed to be due to borate regrouping, i.e. due to transformation of amorphous borates into their crystalline forms [40,46]. Similar strong exothermic effects were reported earlier when studying crystallization of the amorphous cobalt boride resulting from the interaction of sodium borohydride with cobalt salts in aqueous solutions [8], and the following phases of cobalt borate were found among the crystallization products, $Co(BO_2)_2$ [47], $Co_3(BO_3)_2$ [47] and $Co_2B_2O_5$ [8].

In this work powder X-ray diffraction has been used to identify crystalline phases forming in the Co–B–O sample under heating under vacuum at temperatures before and after the borate regrouping transformation. The XRD diffraction patterns recorded for the as-synthesized Co–B–O sample and for this sample after heating at 500, 600 and 700 °C are compared in Fig. 6. In the starting material the XRD pattern shows a broad featureless peak in the region of 30–40° confirming that the sample is amorphous. Prolonged heating of this sample at 500 °C, and even at 600 °C, did not result in any substantial changes in the diffraction pattern. Only at temperatures above the borate regrouping temperature (700 °C) the formation of $Co_2B_2O_5$ phase [42] was observed. No other phases were found whose formation could be expected in the course of reaction of sodium borate alkaline solution with cobalt chloride.

We can conclude, that the Co–B–O compound synthesized in this work constitutes a hydrated amorphous phase of cobalt borate with a composition $2CoO{\cdot}B_2O_3{\cdot}4H_2O$, which crystallizes as $Co_2B_2O_5$ upon heating at elevated temperatures. The formation of crystalline $Co_2B_2O_5$ was also observed in [8] when studying crystallization products of cobalt boride catalysts formed *in situ* from cobalt chloride and sodium borohydride in solutions. Positive IR identification of the amorphous cobalt borate phase suggests its presence in other similar systems as well (Fig. 4), and justifies the purpose of a more detailed study of the catalytic properties of the Co–B–O phase in the reaction of sodium borohydride hydrolysis as described below.

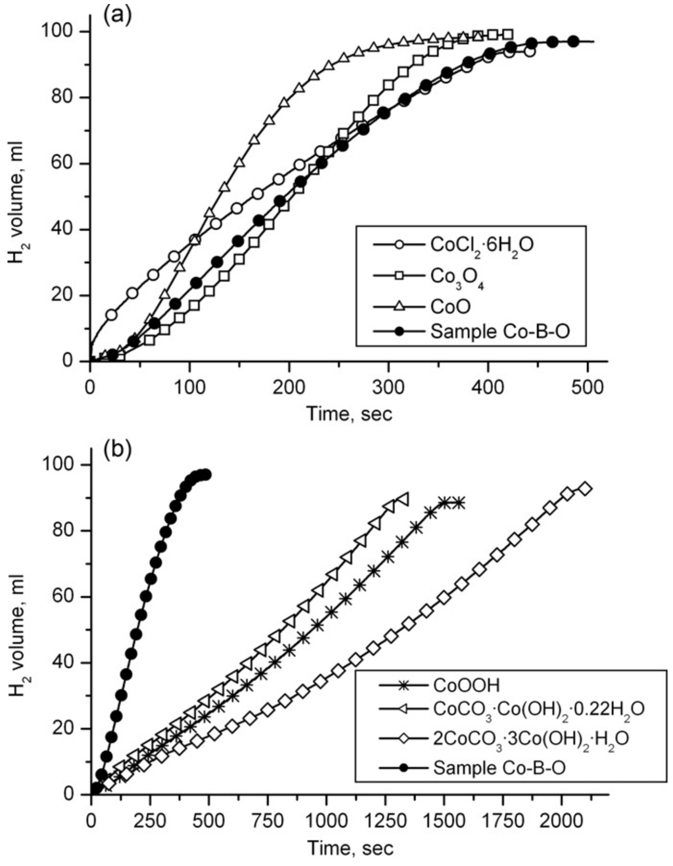

Fig. 7. Catalytic activity of the Co–B–O sample in the hydrolysis of $NaBH_4$ at 40 °C in (a) compared with $CoCl_2{\cdot}6H_2O$, Co_3O_4 and CoO, and in (b) compared with CoOOH, $CoCO_3{\cdot}Co(OH)_2{\cdot}0.22H_2O$ and $2CoCO_3{\cdot}3Co(OH)_2{\cdot}H_2O$.

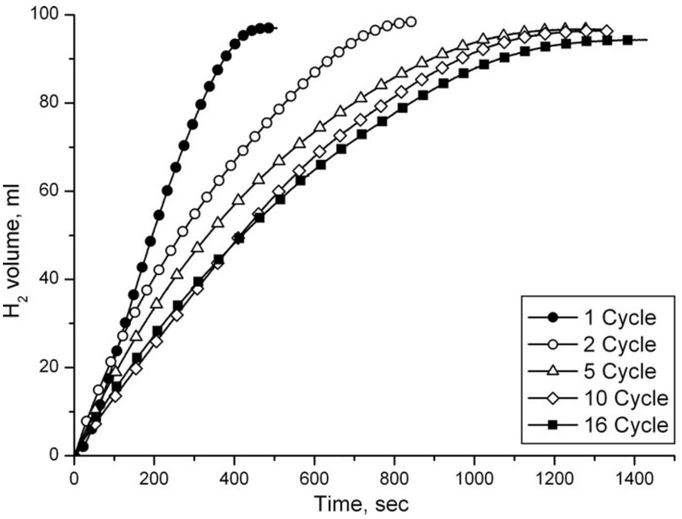

Fig. 8. Stability tests for the Co–B–O sample in hydrolysis of $NaBH_4$ at 40 °C.

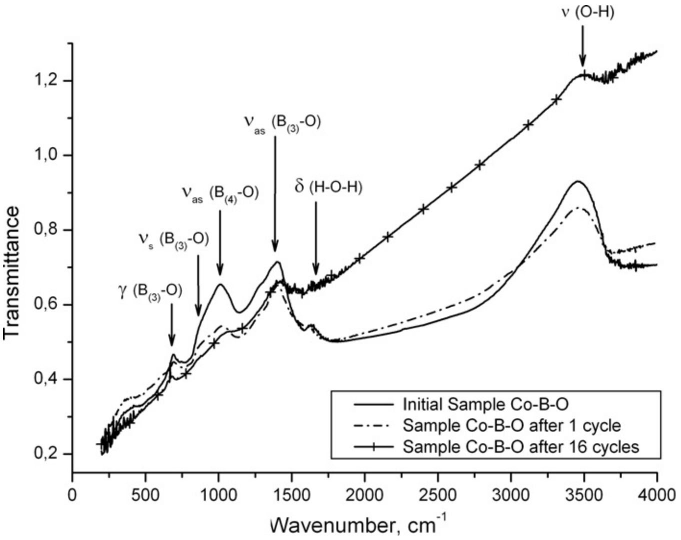

Fig. 9. FTIR spectra of the initial Co–B–O sample, and this sample after 1 and 16 cycles of $NaBH_4$ hydrolysis.

3.2. The catalytic activity of the Co–B–O sample

The kinetic curves of hydrogen release during hydrolysis of $NaBH_4$ in the presence of the synthesized Co–B–O sample and some of the other cobalt compounds are shown in Fig. 7. The catalytic activity of Co–B–O is high and compares favorably with $CoCl_2{\cdot}6H_2O$, CoO and Co_3O_4 compounds which are known to produce the catalytically active phase of cobalt boride *in situ* under the reaction conditions [4,16,20]. The catalytic activity of Co–B–O exceeds considerably the catalytic activities of other cobalt oxide compounds studied, including CoOOH, $CoCO_3{\cdot}Co(OH)_2{\cdot}0.22H_2O$, and $2CoCO_3{\cdot}3Co(OH)_2{\cdot}H_2O$ (Fig. 7b). Also resembling CoO and Co_3O_4, in Co–B–O we observe an activation period during the initial stage of reaction with a very low rate of hydrogen generation. This activation period is determined by the time required for the insoluble cobalt compounds to become reduced into the highly active amorphous phase of cobalt boride [13,18]. This reduction rate correlates with their catalytic activity [20].

In the stability tests performed for the Co–B–O sample the hydrogen generation rate gradually decreases with each hydrolysis cycle (Fig. 8 Fig. 8). After 16 cycles of $NaBH_4$ hydrolysis the Co–B–O sample activity was reduced to about 50% of its initial value. Such behavior is also characteristic of cobalt borides formed *in situ* from $CoCl_2$ and Co_3O_4 in the presence of $NaBH_4$ [18,20,25,26]. This decline in activity has been explained by oxidation of the catalysts' active surfaces and by accumulation of the reaction products [9,14,33].

As noted above, the active catalytic systems shown in Fig. 7a, including $CoCl_2{\cdot}6H_2O$, Co_3O_4, and CoO, tend to rapidly become reduced in the $NaBH_4$ reaction medium to form the active amorphous phases of cobalt borides [4,16,20]. Similarly, the catalytic activity of Co–B–O appears to be the result of its reduction by $NaBH_4$ to form the catalytically active boride phase. In the course of $NaBH_4$ hydrolysis the color of Co–B–O changes from purple to black and the sample becomes ferromagnetic. Chemical analysis of the black Co–B–O sample after the reaction showed 55.60 wt.% Co and 6.76 wt.% B, i.e. the Co:B mole ratio increases from 1.09 to 1.5 after the reaction due to higher cobalt content. In the FTIR spectrum of the tested Co–B–O sample (Fig. 9) the absorption bands corresponding to the starting Co–B–O sample were still present but were significantly less pronounced. After the long-term stability tests of Co–B–O (16 cycles) the absorption band intensities corresponding to borate ions further decreased while the overall level of the absorption increased. This suggests a reduction of Co–B–O borate as it interacts with $NaBH_4$ to form the cobalt-rich phase.

Formation of the new cobalt-containing phase is also confirmed by X-ray diffraction analysis of this sample (Fig. 10). While at room

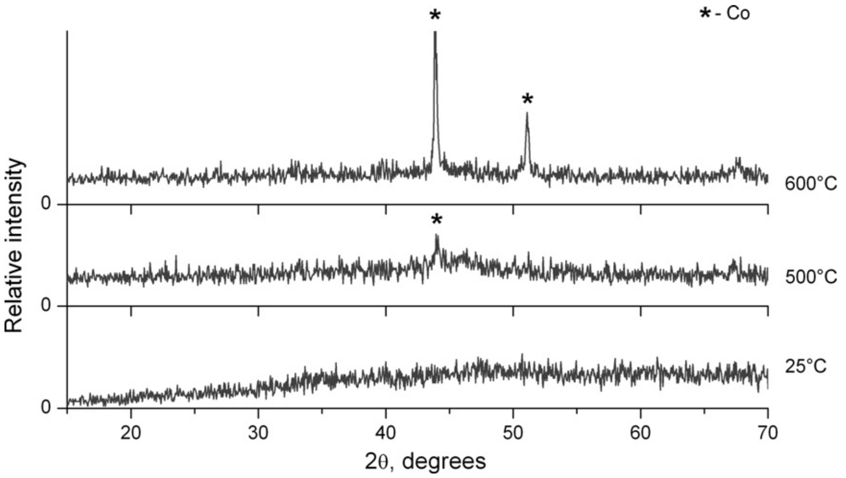

Fig. 10. XRD patterns of the Co–B–O sample tested in $NaBH_4$ hydrolysis and then treated at 25, 500 and 600 °C under vacuum.

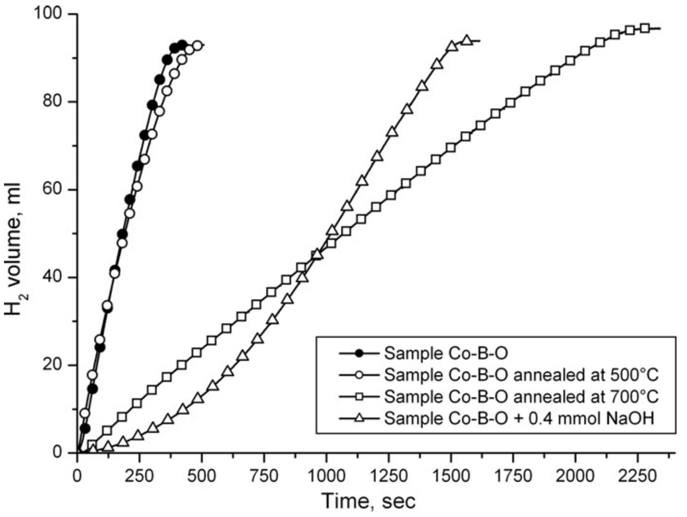

Fig. 11. Catalytic activity of the initial Co–B–O sample and of Co–B–O calcined at 500 °C and 700 °C in the hydrolysis of aqueous (0.12 M $NaBH_4$) and alkaline (0.12 M $NaBH_4$, 0.04 M NaOH) solutions of $NaBH_4$ at 40 °C.

temperature the tested Co–B–O sample was X-ray amorphous, it also remained amorphous upon heating in vacuum up to 500 °C. At 500 °C, however, there appears a peak in the XRD pattern at $2\theta = 44°$ corresponding to (1 1 1) reflection of metallic cobalt with *fcc* cubic crystal structure. As the temperature was further increased to 600 °C there was an increase in intensity of peaks corresponding to metallic cobalt. Thus, on the basis of FTIR spectroscopy and XRD studies, we can conclude that interaction of the Co–B–O sample with the solution of $NaBH_4$ leads to its reduction to form an amorphous cobalt-containing phase. The calcinations of this phase under vacuum to above 500 °C results in crystallized metallic cobalt. This cobalt-containing phase may be either metallic cobalt or cobalt boride, the latter has been shown to oxidize to metallic cobalt by the cobalt borate phase that can be present in the sample [36]. In the $NaBH_4$ medium the cobalt boride phase can be formed as a result of reduction of both cobalt salts and cobalt oxides [4,16,18,20], which is applicable to the Co–B–O case as well.

As shown in Fig. 7, in the aqueous solution of $NaBH_4$ the amorphous Co–B–O sample rapidly reduces to form the catalytically active cobalt-containing phase with the activation period of about 40 s. In additional tests with the Co–B–O sample in the alkaline solution of $NaBH_4$ (0.12 M $NaBH_4$, 0.04 M NaOH) the hydrogen release rate is decreased considerably (Fig. 11), indicating the negative effect of alkali on the formation rate of the catalytically active phase. This observation may be explained by formation of basic compounds of cobalt of low activity (Fig. 7b) upon the contact of cobalt borate with the alkali solution of sodium borohydride.

The effect of the Co–B–O sample crystallization on H_2 generation is negative as well. As can be seen in Fig. 11 a thermal treatment of Co–B–O at 500 °C accompanied by dehydration of the sample (Fig. 5) with preserving its amorphous state (Fig. 6) has no influence on its catalytic activity. At the same time the increase of calcination temperature to 700 °C, when the sample begins to crystallize to form the $Co_2B_2O_5$ phase (Fig. 6), there was observed considerable reduction in the H_2 generation rate.

4. Conclusions

Cobalt compounds demonstrate high catalytic activity in hydrolysis of $NaBH_4$ due to their ability to form the catalytically active cobalt boride phase. Simultaneously with this process, the interaction of cobalt ions with borate anions takes place resulting in the cobalt borate phase which contribution to the overall activity of the catalytic system must be taken into consideration. In this work the amorphous cobalt borate phase, $2CoO{\cdot}B_2O_3{\cdot}4H_2O$, has been synthesized and characterized. The synthesized cobalt borate has been shown to have high catalytic activity in $NaBH_4$ hydrolysis comparable to that of $CoCl_2{\cdot}6H_2O$, Co_3O_4, and CoO. High activity of this cobalt borate has been shown to be due to its reduction in the presence of $NaBH_4$ to form the active cobalt-containing phase, presumably cobalt boride. The use of the alkaline solution of $NaBH_4$ and crystallization of cobalt borate to $Co_2B_2O_5$ under heating at 700 °C both have negative influence on the rate of its reduction to the catalytically active phase, which in turn leads to reduction in the hydrogen release rates.

Acknowledgements

The Russian Foundation for Basic Research (RFBR) is acknowledged for financial support (grants no. 09-08-00505a and no. 09-08-00546a).

References

[1] I.P. Jain, P. Jain, A. Jain, J. Alloys Compd. 503 (2010) 303–339.
[2] L. George, S.K. Saxena, Int. J. Hydrogen Energy 35 (2010) 5454–5470.
[3] D.M.F. Santos, C.A.C. Sequeira, Renewable Sustainable Energy Rev. 15 (2011) 3980–4001.
[4] H.I. Schlesinger, H.C. Brown, A.E. Finholt, J.R. Gilbreath, H.R. Hoekstra, E.K. Hyde, J. Am. Chem. Soc. 75 (1953) 215–219.
[5] V.G. Minkina, S.I. Shabunya, V.I. Kalinin, V.V. Martynenko, A.L. Smirnova, Int. J. Hydrogen Energy 33 (2008) 5629–5635.
[6] S.S. Muir, X. Yao, Int. J Hydrogen Energy 36 (2011) 5983–5997.
[7] B.H. Liu, Z.P. Li, S. Suda, J. Alloys Compd. 468 (2009) 493–498.
[8] A. Garron, D. Swierczynski, S. Bennici, A. Auroux, Int. J. Hydrogen Energy 34 (2009) 1185–1199.
[9] J.H. Kim, K.T. Kim, Y.M. Kang, H.S. Kim, M.S. Song, Y.J. Lee, P.S. Lee, J.Y. Lee, J. Alloys Compd. 379 (2004) 222–227.
[10] S. Özkar, M. Zahmakıran, J. Alloys Compd. 404–406 (2005) 728–731.
[11] V.I. Simagina, P.A. Storozhenko, O.V. Netskina, O.V. Komova, G.V. Odegova, Y.V. Larichev, A.V. Ishchenko, A.M. Ozerova, Catal. Today 138 (2008) 253–259.
[12] Y.V. Larichev, O.V. Netskina, O.V. Komova, V.I. Simagina, Int. J. Hydrogen Energy 35 (2010) 6501–6507.
[13] U.B. Demirci, P. Miele, Phys. Chem. Chem. Phys. 12 (2010) 14651–14665.
[14] J. Andrieux, D. Swierczynski, L. Laversenne, A. Garron, S. Bennici, C. Goutaudier, P. Miele, A. Auroux, B. Bonnetot, Int. J. Hydrogen Energy 34 (2009) 938–951.
[15] J. Andrieux, U.B. Demirci, P. Miele, Catal. Today 170 (2011) 13–19.
[16] L. Damjanovic, S. Bennici, A. Auroux, J. Power Sources 195 (2010) 3284–3292.
[17] B.H. Liu, Z.P. Li, S. Suda, J. Alloys Compd. 415 (2006) 288–293.
[18] O.V. Komova, V.I. Simagina, O.V. Netskina, D.G. Kellerman, G.V. Odegova, A.V. Ishchenko, N.A. Rudina, Catal. Today 138 (2008) 260–265.
[19] L. Damjanovic, M. Majchrzak, S. Bennici, A. Auroux, Int. J. Hydrogen Energy 36 (2011) 1991–1997.
[20] V.I. Simagina, O.V. Komova, A.M. Ozerova, O.V. Netskina, G.V. Odegova, D.G. Kellerman, O.A. Bulavchenko, A.V. Ishchenko, Appl. Catal. A 394 (2011) 86–92.
[21] H. Ma, W. Ji, J. Zhao, J. Liang, J. Chen, J. Alloys Compd. 474 (2009) 584–589.
[22] O. Akdim, R. Chamoun, U.B. Demirci, Y. Zaatar, A. Khoury, P. Miele, Int. J. Hydrogen Energy (2011), doi:10.1016/j.ijhydene.2011.07.051.
[23] S. Bennici, H. Yu, E. Obeid, A. Auroux, Int. J. Hydrogen Energy 36 (2011) 7431–7442.
[24] N. Patel, R. Fernandes, N. Bazzanella, A. Miotello, Catal. Today 170 (2011) 20–26.
[25] Y. Liang, P. Wang, H.B. Dai, J. Alloys Compd. 491 (2010) 359–365.
[26] H. Tian, Q. Guo, D. Xu, J. Power Sources 195 (2010) 2136–2142.
[27] S.U. Jeong, E.A. Cho, S.W. Nam, I.H. Oh, U.H. Jung, S.H. Kim, Int. J. Hydrogen Energy 32 (2007) 1749–1754.
[28] B.H. Liu, Q. Li, Int. J. Hydrogen Energy 33 (2008) 7385–7391.
[29] N. Patel, G. Guella, A. Kale, A. Miotello, B. Patton, C. Zanchetta, L. Mirenghi, P. Rotolo, Appl. Catal. A 323 (2007) 18–24.
[30] Z. Wu, S. Ge, Catal. Commun. 13 (2011) 40–43.
[31] J.C. Walter, A. Zurawski, D. Montgomery, M. Thornburg, S. Revankar, J. Power Sources 179 (2008) 335–339.
[32] N. Patel, R. Fernandes, A. Miotello, J. Catal. 271 (2010) 315–324.
[33] M. Rakap, E.E. Kalu, S. Özkar, J. Alloys Compd. 509 (2011) 7016–7021.
[34] X. Yuan, C. Jia, X.L. Ding, Z.F. Ma, Int. J. Hydrogen Energy (2011), doi:10.1016/j.ijhydene.2011.03.064.
[35] X.L. Ding, X. Yuan, C. Jia, Z.F. Ma, Int. J. Hydrogen Energy 35 (2010) 11077–11084.
[36] G.N. Glavee, K.J. Klabunde, C.M. Sorensen, G.C. Hadjipanayis, Langmuir 8 (1992) 771–773.
[37] A. Corrias, G. Ennas, G. Licheri, G. Marongiu, G. Paschina, Chem. Mater. 2 (1990) 363–366.
[38] H.K. Lin, C.B. Wang, H.C. Chiu, S.H. Chien, Catal. Lett. 86 (2003) 63–68.
[39] G.L. Bezemer, P.B. Radstake, V. Koot, A.J. van Dillen, J.W. Geus, K.P. de Jong, J. Catal. 237 (2006) 291–302.

[40] A.F. Keshan, The Synthesis of Borates in Aqueous Solution and their Investigation, Izd. AN Latv. SSR, Riga, 1955 (in Russian).
[41] T. Mimani, S. Ghosh, Curr. Sci. 78 (2000) 892–896.
[42] J.L.C. Rowsell, N.J. Taylor, L.F. Nazar, J. Solid State Chem. 174 (2003) 189–197.
[43] L. Jun, X. Shuping, G. Shiyang, Spectrochim. Acta A 51 (1995) 519–532.
[44] E.M. Anghel, M. Zaharescu, S. Zuca, J. Mater. Sci. 34 (1999) 3923–3929.
[45] I. Markova-Deneva, J Univ. Chem. Technol. Met. (Sofia) 45 (2010) 351–378.
[46] E. Schwartz, A. Dzene, A. Ievins, J. Therm. Anal. 1 (1969) 279–282.
[47] A.K. Srivastava, S. Madhavi, T.J. White, R.V. Ramanujan, J. Mater. Chem. 15 (2005) 4424–4428.